Journal of Magnetism and Magnetic Materials 588 (2023) 171389

Contents lists available at ScienceDirect

Journal of Magnetism and Magnetic Materials

journal homepage: www.elsevier.com/locate/jmmm

Research article

# Role of the amorphous $SiO_2$/C matrix on the anomalous saturation magnetization of Ni nanoparticles

S.H. Masunaga [a,b,*], V.B. Barbeta [a], R.F. Jardim [b]

[a] Department of Physics, Centro Universitário FEI, Av. Humberto de Alencar Castelo Branco, 3972, São Bernardo do Campo, 09850-901, SP, Brazil
[b] Instituto de Física, Universidade de São Paulo, Rua do Matão, 1371, São Paulo, 05508-090, SP, Brazil

ARTICLE INFO

*Keywords:*
Saturation magnetization
Ni nanoparticles
$SiO_2$/C matrix
Bloch's law

ABSTRACT

Ni nanoparticles (NPs) with a mean diameter ~5 nm, embedded in an amorphous $SiO_2$ and C matrix ($SiO_2$/C) were produced through a modified sol–gel method. Magnetization measurements at temperatures ranging from 2 to 350 K and under an applied magnetic field of 70 kOe showed two different temperature regimes: (i) for temperatures from 2 to 100 K, where an exponential-like decrease in the temperature dependence of the saturation magnetization $M_S(T)$ is observed; and (ii) a slower decrease in $M_S(T)$ with increasing $T$ above 100 K, attributed to spin waves, and obeying the predictions of the Bloch's law. Fittings performed to the data adding appropriate terms to the Bloch's law indicated that the low temperature behavior of $M_S(T)$ can be satisfactorily explained as the result of magnetic contributions from the amorphous $SiO_2$/C matrix and from the surface of the NPs. The high temperature behavior of $M_S(T)$ follows the Bloch's law with an exponent $\alpha = 3/2$ and an increased $B$ value, compared to the Ni bulk.

## 1. Introduction

Metallic nanoparticles (MNPs) have been intensively studied, especially due to their important technological application like, for instance, in bio-medicine [1,2]. Although many properties have been understood through the years, there are some fundamental aspects that are still a matter of intense research and controversy [3,4].

One important aspect for technological application is the influence of coating in MNPs, as well as understanding the temperature ($T$) dependence of their magnetic properties, including here the temperature dependence of saturation magnetization $M_S(T)$. This fundamental problem was theoretically addressed by Bloch almost hundred years ago, and it was described by invoking the propagation of spin waves throughout the magnetic material, with $M_S(T)$ decreasing with increasing temperature [5].

The simplest form of the Bloch's law, that describes the temperature dependence of the zero magnetic field ($H = 0$) spontaneous magnetization $M_S(T)$ is:

$$M_S(T) = M_0\,(1 - BT^{\alpha}), \tag{1}$$

where $M_0$ is the saturation magnetization at $T = 0$ K, $\alpha$ is an exponent that usually takes the value 3/2 for three-dimensional bulk materials, and $B$ is a constant that depends on the exchange integral in the material [5,6].

For the particular case of nickel (Ni) Pauthenet [7] based on a more general spin wave theory proposed by Dyson [8], suggested that $M_S(T)$ of Ni single crystals is well represented when higher power terms are added to the Bloch's law:

$$M_S(T) = M_0\left(1 - BT^{3/2} - a_{5/2}T^{5/2} - a_{7/2}T^{7/2}\right), \tag{2}$$

where the $T^{5/2}$ term is a high order spin wave contribution, and the $T^{7/2}$ term corresponds to the spin-spin collisions. Also, for ferromagnetic Ni, there should be included a susceptibility term $\chi \cdot H$, when $H$ is not zero [7].

For magnetic nanoparticles (NPs) the scenario is certainly more complex and other mechanisms need to be considered. For instance, the $M_S(T)$ behavior of magnetic NPs may differ considerably from that of the bulk due to surface effects, like spin canting, surface spin disorder, broken exchange bonds, interface spin-glass clusters, and spin pinning [9–12]. Also, the $a_{5/2}$ term can be positive, zero or negative, depending on the energy gap and external magnetic field [13].

The experimental results found in literature for magnetic NPs are not consensual, and some researchers have observed that the exponent $\alpha = 3/2$ is maintained in some situations, with alteration of $B$ value, while others have concluded that the $\alpha = 3/2$ exponent is no longer obeyed [14,15]. For instance, the temperature dependence of $M_S$ of ultrafine Fe particles embedded in a $SiO_2$ matrix was found

* Corresponding author at: Instituto de Física, Universidade de São Paulo, Rua do Matão, 1371, São Paulo, 05508-090, SP, Brazil.
*E-mail address:* sueli.masunaga@gmail.com (S.H. Masunaga).

https://doi.org/10.1016/j.jmmm.2023.171389
Received 6 June 2023; Received in revised form 18 September 2023; Accepted 15 October 2023
Available online 17 October 2023

to follow the Bloch's law in a large temperature window, with the usual 3/2 exponent expected for three dimensional (3D) systems, a feature accompanied by a $B$ value around ten times higher than its bulk counterpart. However, at very low temperatures, a strong increase of $M_S$ with decreasing $T$ was observed and attributed to an effect of the NPs size distribution [14].

Experimental results of many other investigations have also indicated a marked exponential-like, low temperature enhancement of $M_S$ in a variety of magnetic compounds, and this feature was associated with different origins. For example, the increase of $M_S(T)$ in the low $T$ regime found in nanostructured Co/Pt was explained by considering changes in the chemical potential of the NPs, which varies with temperature due to a Bose–Einstein condensation of magnons [16].

Some other researchers have tried to explain their exponential-like low $T$ increase of $M_S$ data as the result of an open gap in the NPs phonon energy spectrum, due to the finite size of the nanocrystals [17]. On the other hand, Mørup argued that the uniform mode at low $T$ is predominant in NPs, and instead of an exponential increase of the spontaneous magnetization with decreasing temperature, a linear increase would be expected, suggesting that the low $T$ deviations could be associated with paramagnetic impurities in the samples [18].

The study of the effect of $SiO_2$ coating on magnetic properties of $Fe_3O_4$ NPs, conducted by Larumbe et al. [11], also revealed that only their coated NPs exhibited an exponential-like feature at low temperatures, with the saturation magnetization at $T = 0$ K reaching a value below the uncoated material. This behavior was also related to surface spin disorder that would be greatly enhanced by the NPs silica coating. A similar argumentation was used to explain a low $T$ contribution to the spontaneous magnetization observed in Si coated cobalt NPs [19]. Of particular interest to our purposes is the systematic study conducted in $SiO_2/\gamma$-$Fe_2O_3$ nanocomposites [20]. The authors found that the low temperature fast increase in $M_S(T)$ becomes more evident when the $SiO_2$ content is increased, establishing a correlation between the exponential-like feature in low $T$ magnetization and the $SiO_2$ content.

Within this complex scenario and to shed light in this fundamental problem, we have carefully studied the behavior of the saturation magnetization $M_S(T)$ of Ni NPs embedded in an amorphous $SiO_2$/C matrix in a large range of temperatures and with different Ni concentrations. Therefore, the aim of this work is to verify the application of Bloch's law for Ni NPs, as well as to understand contributions arising from the amorphous $SiO_2$/C matrix content and other magnetic and morphological variables on the low $T$ deviations of the Bloch's law.

## 2. Experimental

Very diluted Ni NPs samples were synthesized through a modified sol–gel method by using tetraethylorthosilicate (TEOS), citric acid, and nickel (II) nitrate, as described in details elsewhere [21]. This process yields a nanocomposite comprising of a ferromagnetic substance (Ni NPs) embedded in an amorphous matrix of silica and carbon ($SiO_2$/C) derived from TEOS. As a result, Ni NPs-$SiO_2$/C samples were obtained, containing spherical NPs measuring ~5 nm in diameter and varying Ni concentration. X-ray powder diffraction (XRD) analysis, provided in the Supplementary Material (SM), indicates the absence of any oxide phases in the nanoparticles (Fig. S1 of SM).

Throughout the series, the concentration of Ni was maintained very low, ranging from 1.9 to 12.8 wt%. For samples containing less than 4.0 wt% Ni, the dipolar interaction can be considered negligibly small [22]. Conversely, for samples containing more than 4.0 wt% Ni, dipolar interaction has been identified, albeit not strong enough to cause a collective spin-glass state [22]. Hence, this Ni NPs series comprises a significant amount of amorphous $SiO_2$/C matrix, making it appropriate for investigating the influence of the amorphous matrix's magnetization on the magnetic properties of our Ni NPs systems.

Further samples of interest for this investigation were also prepared. Nickel oxide NiO NPs were synthesized from a precursor Ni-$SiO_2$/C sample containing 1.9 wt% Ni by subjecting it to a heat treatment performed at 250 °C under $O_2$ atmosphere for 90 min. After the heat treatment in the oxidizing atmosphere, the morphology of the NiO NPs, such as the shape and average particle size, remained unchanged due to the low temperature of the heat treatment. Figure S2 in the Supplementary Material showed the complete oxidation of this sample, as evidenced by the presence of diffraction peaks corresponding only to NiO. Additionally, a sample consisting solely of $SiO_2$ and C was synthesized using the same modified sol–gel technique. This $SiO_2$/C matrix was then mixed with a standard, high purity bulk Ni sample at weight ratios of 95.0:5.0 and 97.5:2.5, respectively.

Magnetization measurements ($M$ vs $T$ and $M$ vs $H$) were carried out using two commercial platforms from Quantum Design: (i) a Superconducting Quantum Interference Device (SQUID) magnetometer; and (ii) a Vibrating Sample Magnetometer (VSM) option of a Physical Property Measurement System (PPMS). The $M$ vs $T$ experiments were conducted in a wide range of temperatures (from 2 to 350 K) and applied magnetic fields as high as 70 kOe. Both Zero-Field-Cooling (ZFC) and Field-Cooling (FC) modes at 70 kOe were measured and found to be reversible. The applied magnetic field of 70 kOe was sufficient to saturate the Ni-NPs samples under investigation. Therefore, the $M$ vs $T$ data taken at 70 kOe are referred as saturation magnetization ($M_S$ vs $T$) in the following sections.

Exclusively for the standard Ni bulk sample, $M$ vs $T$ curves were taken under an applied magnetic field of 10 kOe. The $M$ vs $H$ curves were measured in the magnetic field range of −70 kOe to +70 kOe, at various temperatures following the ZFC process, and only at 5 K after FC process. The FC process was conducted with an applied magnetic field of 50 kOe during sample cooling to 5 K.

## 3. Results and discussion

### 3.1. Bloch's law at high temperatures

Fig. 1 shows a typical temperature dependence of saturation magnetization ($M_S$ vs $T$) curves under an applied magnetic field of 70 kOe for two samples: 1.9 and 12.8 wt% Ni NPs-$SiO_2$/C. The overall data indicate that there are two apparently distinct regimes in the $M_S(T)$ behavior: (i) for low temperatures, roughly up to ~100 K, where an exponential-like fast decrease in $M_S$ with increasing $T$ takes place; and (ii) above 100 K, where a slower, progressive, and smooth decrease in $M_S(T)$ is observed, a feature typically found in a ferromagnetic system under the effect of thermally-induced spin waves.

To certify that the fittings to the Bloch's law is obeyed in a narrower range of temperatures ($T \geq 100$ K), first we have borrowed the data published by Pauthenet for crystalline Ni [7], and also obtained the $M_S$vs $T$ data for polycrystalline Ni samples, where the exponential-like contribution is not perceptible or even absent. The first step was fitting Eq. (2) to the data of Pauthenet [7] for a wider temperature range, roughly from 4 to 300 K, a procedure followed by narrowing the temperature range from 100 to 300 K, observing the quality of the resulting fit. The purpose here was to investigate the effect of narrowing the temperature window of fitting on the $B$ constant value, since generally only $B$ is reported in other studies, and it is the variable of interest.

The $M_S$ vs $T$ data for the Ni crystal are available in Ref. [7], for a temperature range from ~4.2 to ~287 K. The fittings performed using Eq. (2) for the entire temperature range resulted in $B_T = 8.2 \cdot 10^{-6}$ K$^{-3/2}$, and $B_{T \geq 100K} = 6.3 \cdot 10^{-6}$ K$^{-3/2}$ for the narrowed range, roughly from 100 to 300 K. It is important to state that $B$, obtained in Ref. [7] using a different approach, was found to be $B_T = 6.84 \cdot 10^{-6}$ K$^{-3/2}$, a value in line with both above mentioned. In this context, it seems reasonable to consider that a ~17% change in $B$ is

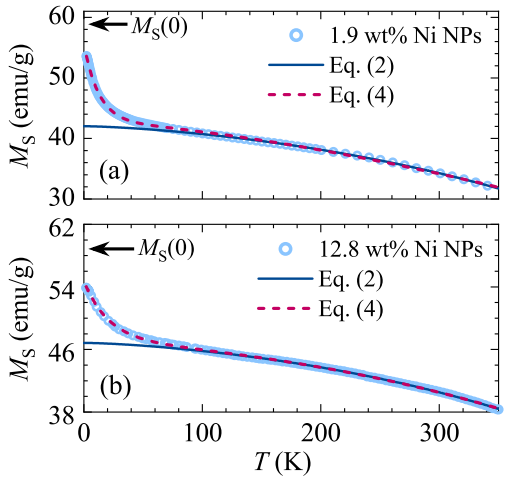


**Fig. 1.** $M_S$ vs $T$ curves for (a) 1.9 and (b) 12.8 wt% Ni NPs samples, taken under an external magnetic field of 70 kOe. The curves exhibit an exponential-like behavior at low temperatures. Similar behavior of $M_S(T)$ data has been observed for all samples listed in Table 1. The arrows indicate the saturation magnetization $M_S(0)$ at $T = 0$ K for bulk Ni.

quite acceptable, when different fitting ranges in the $M_S$ vs $T$ data are used.

For the polycrystalline Ni sample, the curve $M_S$ vs $T$ is presented in Fig. S3 of the Supplementary Material. The fittings performed using Eq. (2) for the whole and narrow temperature ranges resulted in $B_T = 5.6 \cdot 10^{-6}$ K$^{-3/2}$, and $B_{T \geq 100K} = 6.7 \cdot 10^{-6}$ K$^{-3/2}$, respectively. These values differ in less than ~17% and, therefore, it would appear reasonable to consider that even in a narrower temperature range, the fitting does not result in significant changes, since it maintains the same order of magnitude for $B$.

Based on the above results, we consider that it is reliable, for Ni NPs to fit the Bloch's law above 100 K. Therefore, the $M_S(T)$ data above 100 K were fitted by using Eq. (2) for our Ni NPs-$SiO_2$/C samples, and selected results are shown in Fig. 1. Since experimental data from different magnetic NPs systems have shown that the exponent $\alpha = 3/2$ holds [13,14,23–25], and to avoid an excess of free parameters, the exponent $\alpha = 3/2$ was maintained fixed in our fitting procedure.

The relevant parameters obtained from the fitting and necessary for the analysis of the spin-wave stiffness ($D$) are listed in Table 1. We also mention that certain parameters of the fitting as $a_{5/2}$ and $a_{7/2}$, which are not relevant to the discussion, have been omitted from the table for the sake of clarity. The spin wave stiffness constant $D$ is related to the fitting parameter $B$ by:

$$D = \frac{k_B}{4\pi}\left(\frac{2.612\ g\mu_B}{\rho M_0 B}\right)^{2/3}, \tag{3}$$

where $g$ is the Landé $g$-factor, $k_B$ is the Boltzmann constant, $\mu_B$ is the Bohr magneton, $\rho$ is the density, and $M_0$ is the value of $M_S$ at $T = 0$ K and considered here to be 58.858 emu/g [7].

By inspecting the fitted curve above ~100 K in Fig. 1, it is possible to notice that the $M_S(T)$ data of 1.9 and 12.8 wt% Ni NPs-$SiO_2$/C are well described by the Bloch's law, but with an almost four times higher $B$ value (Table 1) when compared with the one obtained in the bulk Ni of $6.84 \cdot 10^{-6}$ K$^{-3/2}$ [7]. Higher $B$ values correspond to lower spin wave stiffness constant $D$, a feature commonly attributed to size effects due to the increased surface spins contribution who are poorly correlated to the core, as has been frequently argued to occur in different nanostructured systems [14,26–28]. Also, the $M_0$ values obtained for NPs are slightly lower than those of the bulk material, but this is a common feature seen in nanostructured systems [11,13,26,29,30]. The difference between the experimental $M_0$ values obtained for Ni NPs-$SiO_2$/C samples (represented by the solid line extrapolated to 0 K) and the expected saturation magnetization at $T = 0$ K for bulk Ni (indicated by arrows) can be visualized in Fig. 1.

**Table 1**
Saturation magnetization $M_0$ and parameter $B$ obtained by fitting Eq. (2) to the high temperature data, for different Ni concentrations. The spin wave stiffness constant $D$ was obtained using Eq. (3).

| Ni (wt%) | $M_0$ (emu/g) | $B$ ($10^{-6}$ K$^{-3/2}$) | $D$ (meV Å$^2$) |
|---|---|---|---|
| 1.9 | 42 | 25 | 174 |
| 2.7 | 50 | 21 | 195 |
| 4.0 | 51 | 25 | 174 |
| 7.9 | 38 | 18 | 216 |
| 12.8 | 47 | 22 | 189 |

It is worth noting that depending on the technique employed for determining the spin wave stiffness constant $D$ for bulk materials, different values are frequently found. For instance, the estimated $D$ values using our $M_S(T)$ data were consistently smaller than that obtained for Ni bulk at low temperatures using neutron spectroscopy ($D \sim 400$ meV Å$^2$) [31]. However, the $B$ values listed in Table 1 are in line with that found elsewhere for Ni NPs of $20 \cdot 10^{-6}$ K$^{-3/2}$ [13], which are close to one order of magnitude higher than the value obtained for Ni bulk. Such a discrepancy was justified by the occurrence of a thin NiO layer covering the Ni NPs and/or due to a disordered surface layer [13].

### 3.2. Deviation of Bloch's law at low temperatures

Let us move now to the low $T$ regime of $M_S(T)$, where the exponential-like behavior is clearly observed. We would like to emphasize that this kind of $M_S$ dependence, as shown in Fig. 1 below ~100 K, has been reported in a variety of magnetic systems comprised of NPs: $\gamma - Fe_2O_3$ [20,32,33], $NiFe_2O_4$ [17,34], $BiFeO_3$–CuO nanocomposite [35], $Fe_3O_4$ [11], $CoFe_2O_4$ [28], $MnFe_2O_4$ [27], Ni/NiO [25] among others. Besides, such a feature seems to be independent of the presence (or not) of coatings and coating types, further indicating that size effects may play a role in the anomalous behavior of $M_S(T)$. In some cases, experimentally determined $M_S$ towards $T = 0$ K exhibits little deviation from the asymptotically value $M_0$, with a small change in the slope of the $M_S(T)$ curve, and sometimes such a feature is just disregarded [36–38]. Therefore, the low $T$ feature in $M_S(T)$ curves seems to be more general, and fittings to the canonical Bloch's temperature dependence of saturation magnetization (Eq. (1) or Eq. (2)) are clearly affected by it.

The abrupt increase in $M_S(T)$ at low $T$ leading to a clear deviation from Bloch's law in magnetic NPs has also been attributed to surface spin freezing [27,39–41]. To account for this experimentally observed deviation, effects arising from both finite-size and surface spins ($M_{shell}$) have been incorporated to the Bloch's law as an additional contribution. This surface contribution has being then modeled by considering a phenomenological exponential term [27,28,42], and the modified Bloch's equation takes the form:

$$M_S(T) = M_0\left(1 - BT^{3/2} - \cdots\right) + M_{shell}\exp\left(-\frac{T}{T_f}\right), \tag{4}$$

where $M_{shell}$ corresponds to the shell magnetization of the small granules, and $T_f$, the spin-freezing temperature of the shell. The extra term in Eq. (4) accounts for contributions to $M_S(T)$ arising from the surface of the NPs, as well as material characteristics and NPs size. According to Eq. (4), the surface contribution to the magnetization $M_{shell}$ approaches zero as the temperature increases.

The fitting of Eq. (4) to the $M_S$ vs $T$ data is shown in Fig. 1 (red dashed line), and the fitting parameters are listed in Table 2. From the extracted parameters of the fitting, one can estimate the thickness of the shell ($t_{shell}$) through the relationship [42]:

$$t_{shell} = \left(1 - \gamma^{1/3}\right) r, \tag{5}$$

**Table 2**
The parameters $M_0$, $B$, $M_{shell}$, and $T_f$ were obtained by fitting Eq. (4) to the $M_S$ vs $T$ data for samples with varying concentrations of Ni NPs. The shell thickness $t_{shell}$ was estimated using Eq. (5).

| Ni (wt%) | $M_0$ (emu/g) | $B$ ($10^{-6}$ K$^{-3/2}$) | $M_{shell}$ (emu/g) | $T_f$ (K) | $t_{shell}$ (nm) |
|---|---|---|---|---|---|
| 1.9 | 42 | 37 | 13 | 13 | 0.2 |
| 2.7 | 51 | 29 | 7.8 | 13 | 0.1 |
| 4.0 | 52 | 28 | 7.1 | 15 | 0.1 |
| 7.9 | 38 | 21 | 5,7 | 21 | 0.2 |
| 12.8 | 47 | 23 | 7.7 | 21 | 0.1 |

where $\gamma = M_{core}/(M_{core}+M_{shell})$, $r$ is the radius of NPs, and $M_{core} = M_0$.

The $t_{shell}$ values (Table 2) extracted from the fitting procedure are quite reasonable, considering the ~5 nm diameter size of the Ni NPs. Still, this result does not rule out a contribution to $M(T)$ of the amorphous $SiO_2$/C matrix, as pointed out in Refs. [11] and [20]. In addition, some authors have claimed that under specific circumstances, silicon itself can exhibit magnetic properties [43,44]. For instance, the authors of Ref. [43] argued that silicon can show appreciable magnetic properties when its surfaces are etched first with HF and then with KOH. On the other hand, Grace et al. [45] proposed that some results could be explained based on the presence of contaminants from pyrex beakers and impurities in solvents, such as KOH, used during the etching process of silicon.

To deepen our understanding of the eventual influence of the $SiO_2$/C matrix on $M(T)$, chunks of high-purity, polycrystalline Ni were mixed with the amorphous $SiO_2$/C matrix at two weight ratios of the matrix material, 95.0 wt% and 97.5 wt%, and characterized by magnetic measurements. The $M_S(T)$ curves of these two samples, taken under an applied magnetic field of 70 kOe, are displayed in Fig. 2. Two important features of these $M_S(T)$ curves at low $T$ are of interest: (i) an exponential-like increase in both $M_S(T)$ curves; and (ii) higher $M_S(T)$ values, above the expected saturation magnetization $M_S(0) \sim 58.9$ emu/g at $T = 0$ K for bulk Ni, as indicated by arrows in Fig. 2. We emphasize here that it was not feasible to exclusively measure the magnetic properties of the amorphous $SiO_2$/C matrix $M_{matrix}(T)$ at low temperatures. The $M_{matrix}(T)$ data exhibited inconsistencies when different runs were compared, possibly due to limitations in the measurement system or measurement artifacts. In any event, the data of the two samples displayed in the inset of Fig. 2 indicate that the $M_S(T)$ behavior at low $T$ undergoes minimal changes when the mass proportion of Ni chunk is reduced by half, indicating a more consistent outcome for the magnetization of the $SiO_2$/C matrix.

Fitting the data of the Ni chunk mixed with the amorphous $SiO_2$/C matrix to the Bloch's law (Eq. (2) in Fig. 2), in the range 100 to 350 K, resulted in $B_{T\geq 100K} = 6.0 \cdot 10^{-6}$ K$^{-3/2}$, a value similar to those obtained for poly and single crystalline Ni samples already mentioned in Section 3.1. Such a result strongly suggests that the contribution of the amorphous $SiO_2$/C matrix to $M_S(T)$ at temperatures higher than ~100 K can be disregarded in our analysis. On the other hand, fitting of Eq. (4) to $M_S$ vs $T$ data for the same samples resulted in the parameters displayed in Table 3.

To conduct this new fitting procedure, we renamed the parameters $M_{shell}$ to $M_{matrix}$ and $T_f$ to $T_{matrix}$ of Eq. (4). It is important to reiterate that we generally quantify the magnetization in terms of the amount of ferromagnetic material present in a given sample, which is Ni in our case, assuming that other constituents exhibit negligible magnetization. As a result, significant $M_{shell}$ values of 4.9 and 6.7 emu/$g_{Ni}$ were obtained through fitting procedure of Eq. (4), as listed in Table 3. After properly correcting the units for $M_{matrix}$, the corresponding values of 0.12 and 0.34 emu/$g_{matrix}$ were estimated for an applied magnetic field of 70 kOe, as presented in Table 3.

Upon evaluating the values of $M_{matrix}$ listed in Table 3 and $M_{shell}$ in Table 2, it becomes clear that the approach results in a significant contribution to $M_S(T)$ at low $T$ of the amorphous $SiO_2$/C matrix, when

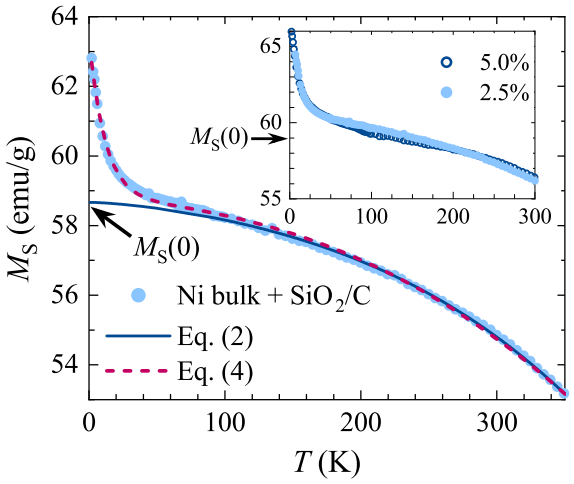


**Fig. 2.** $M_S$ vs $T$ curve obtained for a sample consisting of a chunk of polycrystalline Ni mixed with the $SiO_2$/C matrix, under an applied magnetic field of 70 kOe. The continuous and dotted lines show the fittings obtained using Eqs. (2) and (4), respectively. The inset displays a collapse of the $M_S$ results, achieved by considering a temperature variation of ±2.5 K and a magnetization variation of ±2.2 emu/g for the two $SiO_2$/C matrix/Ni proportions of 97.5:2.5 and 95.0:5.0. The collapse of both curves demonstrates a consistent low temperatures behavior in the $M_S$ vs $T$ results. The arrows indicate the saturation magnetization $M_S(0)$ at $T = 0$ K for bulk Ni.

**Table 3**
The resulting parameters from fitting Eq. (4) to the data shown in Fig. 2, where the terms $M_{shell}$ and $T_f$ were renamed to $M_{matrix}$ and $T_{matrix}$, respectively. The corresponding $M_{matrix}$ values in emu/$g_{matrix}$ are also given in the last column.

| Ni (wt%) | $M_{matrix}$ (emu/$g_{Ni}$) | $T_{matrix}$ (K) | $M_{matrix}$ (emu/$g_{matrix}$) |
|---|---|---|---|
| 2.5 | 4.9 | 12 | 0.12 |
| 5.0 | 6.7 | 15 | 0.34 |

it is expressed in emu/$g_{Ni}$. Consequently, the magnetic contribution of the $SiO_2$/C matrix, independently of its origin, has to be considered to the analysis, despite the apparently reasonable results for $t_{shell}$ shown in Table 2.

A similar increase in $M_S$ at low $T$ for Ni ferrite samples [17], produced by a method similar applied by us to synthesized our Ni NPs, was attributed to the presence of paramagnetic impurities, that are activated at low temperatures and high magnetic fields [18]. Despite this possibility, some studies have indicated that silica $SiO_2$ itself may exhibit appreciable magnetism due to defects or dopants, such as nitrogen or carbon, and consequently, magnetic hysteresis and an exponential increase in its $M_S(T)$ at low $T$ [46]. However, a simple comparison between curves displayed in Figs. 1 and 2 indicates that a large contribution to the upturn in the $M_S(T)$ data comes from the magnetic signal or contribution of the amorphous $SiO_2$/C matrix in the case of Ni NPs samples. Moreover, as discussed in Ref. [20], a precise correlation between the exponential enhancement of $M_S(T)$ at low $T$ and the concentration of $SiO_2/\gamma - Fe_2O_3$ nanocomposites has been established. Specifically, it was shown that the magnitude of the exponential behavior is magnified further with increasing $SiO_2$ content above a threshold value of ~13 wt% $SiO_2$. Additional investigation on nanomaterials featuring $SiO_2$ concentrations exceeding ~13 wt% $SiO_2$ have revealed a marked enhancement of $M_S(T)$ at low $T$. For instance, studies conducted on $NiFe_2O_4$ [17] and $CoFe_2O_4$ [47] in $SiO_2$ have shown a clear exponential-like increase in experimental curves of $M_S(T)$ with decreasing temperature.

### 3.3. Complete model at low temperatures

Comparing the values of $M_{matrix}$ (in emu/$g_{Ni}$) in Table 3 with $M_{shell}$ values in Table 2, it is possible to notice that the former are smaller than

**Table 4**
Parameters obtained from the fittings of $M_S$ vs $T$ curves (Fig. 1) using Eq. (6). The values of $t_{shell}$ were obtained using Eq. (5).

| Ni (wt%) | $M_0$ (emu/$g_{Ni}$) | $B$ ($10^{-6}$ $K^{-3/2}$) | $M_{matrix}$ (emu/$g_{matrix}$) | $T_{matrix}$ (K) | $M_{shell}$ (emu/$g_{Ni}$) | $T_f$ (K) | $t_{shell}$ (nm) |
|---|---|---|---|---|---|---|---|
| 1.9 | 41 | 15 | 0.12 | 8.4 | 5.1 | 51 | 0.08 |
| 2.7 | 50 | 18 | 0.16 | 8.5 | 3.2 | 35 | 0.05 |
| 4.0 | 51 | 23 | 0.22 | 11 | 2.8 | 40 | 0.04 |
| 7.9 | 38 | 16 | 0.32 | 14 | 2.6 | 48 | 0.06 |
| 12.8 | 47 | 16 | 0.40 | 11 | 5.6 | 30 | 0.10 |

the latter, indicating that only the matrix contribution is insufficient to account for the $M_S(T)$ results. The values of $T_f$ and $T_{matrix}$ displayed in Tables 2 and 3, respectively, were found to be very similar, further indicating that it is important to add the magnetic contribution of the amorphous $SiO_2$/C matrix to $M_S(T)$ in our analysis. Therefore, the proposition is to rewrite Eq. (4) and sum to the Bloch's law a phenomenological exponential term, as follows:

$$M_S(T) = M_0\left(1 - BT^{3/2} - a_{5/2}T^{5/2} - a_{7/2}T^{7/2}\right) + M_{shell}\exp\left(-\frac{T}{T_f}\right) + M_{matrix}\exp\left(-\frac{T}{T_{matrix}}\right). \quad (6)$$

To increase the robustness of our analysis, we imposed certain constraints to the fitting parameters of Eq. (6). Specifically, we limited the range of $M_{shell}$ to 0.1–0.4 emu/$g_{matrix}$ and set a maximum value of 15 K for $T_{matrix}$, based on the parameters listed in Table 3. By fitting the $M_S$ vs $T$ data for Ni NPs samples using Eq. (6) we obtained the parameters shown in Table 4. The $M_0$ values agree well with the fitting results obtained by using different equations written above, as already mentioned and shown in Tables 1 and 2. Compared to their bulk counterparts, the lower values of experimentally determined $M_0$ of NPs are generally attributed to surface phenomena. This includes the spin canting phenomenon induced by the broken symmetry or the reduced coordination and broken exchange at the surface of tiny magnetic NPs [16]. The $M_{matrix}$ and $T_{matrix}$ values for different samples are also in good agreement with each other, lending credence to the fitting procedure employed.

The results displayed in Table 4 also indicate that both $M_{shell}$ and $M_{matrix}$ contribute to the upturn of $M(T)$ below ~100 K. The new estimates for $t_{shell}$ using Eq. (5), which range from 0.04 to 0.10 nm, are consistent with the value of 0.05 nm obtained for $Ni_{1-x}Fe_x$ NPs of a similar size [42]. As anticipated for samples with similar size, the values of $M_{shell}$, varying from 2.6 to 5.6 emu/$g_{Ni}$, are in good agreement across distinct samples and appear to remain little affected by weak dipolar interaction between granules. Comparing the newly estimated values of $B$ with those listed in Tables 1 and 2, a marginal decrease was observed. In any event, the $B$ values displayed in Table 4 remain larger than those expected for bulk Ni, owing to the presence of an energy gap in the spin-wave spectrum [39].

It is noteworthy that the magnetic contribution of the amorphous $SiO_2$/C matrix to $M_S(T)$ is negligible for $T \geq 100$ K, and the portion range of the matrix magnetization to $M_S(T)$ lies between ~0.4% and 1.8%. These small contributions to $M_S(T)$ reinforce the initial argument that fitting of $M_S$ vs $T$ data above 100 K by using the Bloch's law without considering the matrix and shell contribution is reliable. Moreover, the similar values of $B$, as listed in Tables 1 and 4, further indicate that the impact of the shell magnetization and matrix contribution to $M_S(T)$ can be disregarded in the fitting process for $T \geq 100$ K.

Another source for the deviation of $M_S(T)$ data at low $T$, not yet discussed, could be related to the presence of an oxidized surface layer in NPs, a phenomenon related to the metallic character of the Ni NPs.

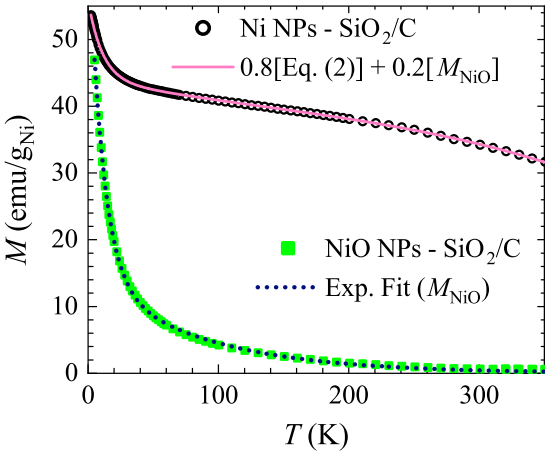


**Fig. 3.** $M$ vs $T$ curves, obtained under 70 kOe, for the as-prepared 1.9 wt% Ni nanoparticle sample (○), as well as for the same sample after heat treatment in an $O_2$ atmosphere (□). The magnetization of NiO NPs ($M_{NiO}$) is effectively fitted by an exponential equation (indicated by the dotted line). The solid line represents the fitting achieved through a weighted sum of Eq. (2) and $M_{NiO}$.

To test this hypothesis, the $M$ vs $T$ curve was obtained under 70 kOe for the NiO NPs-$SiO_2$/C sample. The $M$ vs $T$ curve of this oxidized sample exhibited a much more pronounced increase in the exponential component of $M(T)$ at low temperatures, as displayed in Fig. 3. This result can be compared with a study conducted on Ni NPs coated by NiO, where an exponential-like increase at low temperatures was also observed [25]. Nevertheless, if we attribute the abrupt increase in $M_S(T)$ at low $T$ to the oxidize shell, it would imply that approximately 20 wt% of NiO is present in the sample (for detailed estimation, please refer to the Supplementary Material). As an alternative analysis, in order to account for the lower $M_0$ values observed in our Ni NPs in comparison to the bulk material, a wt% NiO content ranging from 30% to 40% would be required to be present in our samples. These percentages of Ni oxide certainly would be detected, for instance, by XRD analysis, a feature absent in our XRD diagrams (Fig. S1 in SM).

On the other hand, an alternative approach to infer about the occurrence of an oxidized layer in our samples, comprised of antiferromagnetic AFM NiO on the surface of ferromagnetic FM Ni NPs, is through the phenomenon known as exchange bias (EB), i.e., when two magnetic materials are coupled together by the exchange interaction [48]. The occurrence of EB can be identified through magnetic hysteresis loops obtained after the FC process. An illustration of these loops is provided in the inset of Fig. 4 for two representative samples, namely 4.0 and 7.9 wt% Ni NPs.

The inset of Fig. 4 displays the magnetization isotherms ($M$ vs $H$) obtained after the ZFC and FC ($H$= 50 kOe) processes. The hysteresis loops were found to be symmetric about zero field axis with no shift via EB, suggesting that Ni particles are free from an oxide layer. Comparing the magnetization isotherms obtained after the ZFC and FC, under 50 kOe and at 5 K, no evidence of EB was observed for

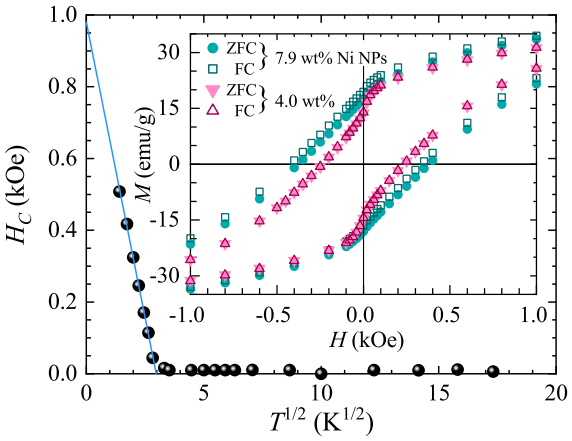


**Fig. 4.** $H_C$ vs $T^{1/2}$ for 7.9 wt% Ni NPs sample. The inset shows the expanded view of hysteresis loops taken at 5 K, after ZFC and FC (50 kOe) processes for 4.0 and 7.9 wt% Ni NPs samples.

samples containing 1.9, 2.7, and 4.0 wt% Ni NPs, as depicted in the inset of Fig. 4, exemplified by the 4.0 wt% sample. For these three samples, the $M$ vs $H$ curves after the ZFC and FC processes were indistinguishable, further supporting that an oxidized layer must be absent in these materials.

For 7.9 wt% and 12.8 wt% samples, exchange bias fields $H_{EB}$ of ~45 and ~150 Oe, respectively, were measured from curves similar to those in the inset of Fig. 4. These values of $H_{EB}$ are relatively small when compared to the estimated $H_{CO} \sim 1$ kOe, for the coercive field of Ni NPs at 0 K. $H_{C0}$ was extracted from the $H_C$ vs $T^{1/2}$ dependence in the region of the Ni NPs-$SiO_2$/C's blocking regime [49], as shown in Fig. 4. Therefore, it is unlikely that the presence of an oxidized layer on the surface of the Ni NPs would be the dominant contribution for the exponential-like behavior of $M_S(T)$ at low $T$, provided that other samples without exhibiting exchange bias display similar characteristics. Moreover, the occurrence of the exchange bias phenomenon is not exclusive to fine particles with a ferromagnetic (FM)-antiferromagnetic (AF) core–shell morphology. Uncoated fine particles may also exhibit EB due to the presence of disordered spins on the surface [50].

We also mention that deviations from the Bloch's law at low temperatures, observed in experimental $M_S(T)$ data for nanostructured systems, has equally been attributed to Bose–Einstein Condensation (BEC) of magnons. The confinement of magnons in tiny NPs is responsible for inducing a gap in the energy spectrum [51], and when confined in small NPs, magnon wave vectors are quantized, resulting in an energy gap between allowed lowest states [16]. In this case, an upturn in magnetization is theoretically expected to occur at the BEC temperature ($T_{BEC}$), resulting in a change in the Bloch's $B$ coefficients.

As far as $T_{BEC}$ is concerned, it is predicted to occur at temperatures below the blocking temperature ($T_B$) and being proportional to the gap temperature $T_{\text{gap}}$, which for a given nanomaterial can be estimated by:

$$T_{\text{gap}} = \frac{3J\pi^2 a^2}{k_B d^2}, \tag{7}$$

where $a$ is the lattice spacing, $J$ the exchange constant, and $k_B$ the Boltzmann constant [52]. We utilized, for Ni, the values $a = 0.352$ nm and $J = 0.34 k_B T_C \sim 3 \cdot 10^{-14}$ erg [53]. For Ni NPs-$SiO_2$/C samples, the experimentally determined $T_B$ were found to range between 7.5 and 16.0 K and the estimated values of $T_{\text{gap}}$ between 24 and 41 K. As the magnetization of the Ni NPs-$SiO_2$/C samples increases abruptly below ~50 K, it is not possible to observe the upturn that would occur below this temperature, being masked by the exponential signal of the surface and matrix.

Therefore, from the previous discussion, it seems reasonable to consider that the low temperature departure from the expected behavior of $M_S(T)$ should be caused by surface disorder as well as a matrix contribution. The origin of the matrix contribution is not clear, and could be the result of a induced $SiO_2$ magnetism or the presence of paramagnetic impurities, although this latter seems to be less probable.

## 4. Conclusions

The saturation magnetization $M_S(T)$ of diluted Ni NPs, embedded in an amorphous $SiO_2$ and C matrix ($SiO_2$/C), were studied through magnetization measurements in an applied magnetic field of 70 kOe and in a temperature range from 5 to 300 K. We have tested our $M_S(T)$ data by using the Bloch's law and have detected two temperature windows in which it manifests in different ways: (i) from ~5 to ~100 K, where an anomalous exponential-like decrease in $M_S(T)$ is observed, and (ii) for temperatures higher than ~100 K, where a progressive, smooth decrease in $M_S(T)$ takes place. In order to evaluate these two behaviors in the light of Bloch's law, we have listed at least five different mechanisms that could be responsible for the low temperature departure of Bloch's law: (i) surface disorder, due spin canting and resulting in spin-freezing; (ii) a magnetic contribution from the $SiO_2$/C matrix; (iii) the presence of an oxide NiO surface layer in the NPs; (iv) Bose–Einstein condensation of magnons; and (v) presence of paramagnetic impurities within the NPs. From our experimental results, combined with an analysis made by adding extra terms to the Bloch's law, we have found that the anomalous exponential-like decrease of $M_S(T)$ is the result of two contributions arising from a disordered surface layer and the amorphous $SiO_2$/C matrix. We also found that $M_S(T)$, for temperatures higher than ~100 K, is well described by the Bloch's law with an increased value of $B$ and an exponent $\alpha = 3/2$.

## CRediT authorship contribution statement

**S.H. Masunaga:** Conceptualization, Investigation, Visualization, Formal analysis and Writing – original draft. **V.B. Barbeta:** Conceptualization, Formal analysis, Writing – original draft. **R.F. Jardim:** Conceptualization, Resources, Supervision, Funding acquisition.

## Declaration of competing interest

The authors declare that they have no known competing financial interests or personal relationships that could have appeared to influence the work reported in this paper.

## Data availability

Data will be made available on request.

## Acknowledgments

This work was supported in part by the Brazilian agency Fundação de Amparo à Pesquisa do Estado de São Paulo (FAPESP under Grant No. 2013/07296-2, 2019/26141-6, and 2022/10874-7), and CNPq (Grant No. 301463/2019-0). The authors are indebted to N. Dilley and J. O'Brien for performing the magnetic measurements in the Ni polycrystalline sample.

## Appendix A. Supplementary material

Supplementary material related to this article can be found online at https://doi.org/10.1016/j.jmmm.2023.171389.

## References


[1] S. Pedroso-Santana, N. Fleitas-Salazar, The use of capping agents in the stabilization and functionalization of metallic nanoparticles for biomedical applications, Part. Part. Syst. Characterization 40 (2) (2023) 2200146, http://dx.doi.org/10.1002/ppsc.202200146.

[2] K. Bhardwaj, C. Chopra, P. Bhardwaj, D.S. Dhanjal, R. Singh, A. Najda, N. Cruz-Martins, S. Singh, R. Sharma, K. Kuča, et al., Biogenic metallic nanoparticles from seed extracts: Characteristics, properties, and applications, J. Nanomater. 2022 (2022) http://dx.doi.org/10.1155/2022/2271278.

[3] N.J. Rommelfanger, Z. Ou, C.H. Keck, G. Hong, Differential heating of metal nanostructures at radio frequencies, Phys. Rev. A 15 (2021) 054007, http://dx.doi.org/10.1103/PhysRevApplied.15.054007.

[4] L. Lin, X. Peng, E. Voirin, B. Donnio, M.V. Rastei, B. Vileno, J.-L. Gallani, Influence of the crystallinity of silver nanoparticles on their magnetic properties, Helv. Chim. Acta 106 (3) (2023) e202200165, http://dx.doi.org/10.1002/hlca.202200165.

[5] F. Bloch, Zur theorie des ferromagnetismus, Zeitschrift Für Phys. 61 (3–4) (1930) 206–219, http://dx.doi.org/10.1007/BF01339661.

[6] C. Caizer, Deviations from Bloch law in the case of surfacted nanoparticles, Appl. Phys. A 80 (2005) 1745–1751, http://dx.doi.org/10.1007/s00339-003-2471-3.

[7] R. Pauthenet, Spin-waves in nickel, iron, and yttrium-iron garnet, J. Appl. Phys. 53 (3) (1982) 2029–2031, http://dx.doi.org/10.1063/1.330694.

[8] F.J. Dyson, General theory of spin-wave interactions, Phys. Rev. 102 (1956) 1217–1230, http://dx.doi.org/10.1103/PhysRev.102.1217.

[9] Y. Chen, K. Maaz, S. Lyu, Y. Cheng, J. Liu, Fabrication and temperature dependent magnetic properties of Co – Ni nanotube arrays, Physica E 110 (2019) 123–126, http://dx.doi.org/10.1016/j.physe.2019.02.004.

[10] I.M. Obaidat, C. Nayek, K. Manna, Investigating the role of shell thickness and field cooling on saturation magnetization and its temperature dependence in $Fe_3O_4/\gamma - Fe_2O_3$ core/shell nanoparticles, Appl. Sci. 7 (12) (2017) http://dx.doi.org/10.3390/app7121269.

[11] S. Larumbe, C. Gómez-Polo, J.I. Pérez-Landazábal, J.M. Pastor, Effect of a $SiO_2$ coating on the magnetic properties of $Fe_3O_4$ nanoparticles, J. Phys.: Condens. Matter 24 (26) (2012) 266007, http://dx.doi.org/10.1088/0953-8984/24/26/266007.

[12] M.P. Proenca, C.T. Sousa, A.M. Pereira, P.B. Tavares, J. Ventura, M. Vazquez, J.P. Araujo, Size and surface effects on the magnetic properties of NiO nanoparticles, Phys. Chem. Chem. Phys. 13 (20) (2011) 9561–9567, http://dx.doi.org/10.1039/C1CP00036E, Publisher: The Royal Society of Chemistry.

[13] S. Vitta, Nonlinear spin wave magnetization of solution synthesized Ni nanoparticles, J. Appl. Phys. 101 (6) (2007) 063901, http://dx.doi.org/10.1063/1.2710437.

[14] G. Xiao, C. Chien, Temperature dependence of spontaneous magnetization of ultrafine Fe particles in $Fe - SiO_2$ granular solids, J. Appl. Phys. 61 (8) (1987) 3308–3310, http://dx.doi.org/10.1063/1.338891.

[15] D. Zhang, K.J. Klabunde, C.M. Sorensen, G.C. Hadjipanayis, Magnetization temperature dependence in iron nanoparticles, Phys. Rev. B 58 (1998) 14167–14170, http://dx.doi.org/10.1103/PhysRevB.58.14167.

[16] E. Della Torre, L.H. Bennett, R.E. Watson, Extension of the Bloch $T^{3/2}$ law to magnetic nanostructures: Bose-Einstein condensation, Phys. Rev. Lett. 94 (2005) 147210, http://dx.doi.org/10.1103/PhysRevLett.94.147210.

[17] K. Mandal, S. Mitra, P.A. Kumar, Deviation from Bloch $T^{3/2}$ law in ferrite nanoparticles, Europhys. Lett. 75 (4) (2006) 618, http://dx.doi.org/10.1209/epl/i2006-10148-y.

[18] S. Mørup, Comment on "deviation from the Bloch $T^{3/2}$ law in ferrite nanoparticles" by K. Mandal et al, Europhys. Lett. 77 (2) (2007) 27003, http://dx.doi.org/10.1209/0295-5075/77/27003.

[19] A. Eggeman, A. Petford-Long, P. Dobson, J. Wiggins, T. Bromwich, R. Dunin-Borkowski, T. Kasama, Synthesis and characterisation of silica encapsulated cobalt nanoparticles and nanoparticle chains, J. Magn. Magn. Mater. 301 (2) (2006) 336–342, http://dx.doi.org/10.1016/j.jmmm.2005.07.022.

[20] D. Li, W.Y. Teoh, R.C. Woodward, J.D. Cashion, C. Selomulya, R. Amal, Evolution of morphology and magnetic properties in silica/maghemite nanocomposites, J. Phys. Chem. C 113 (28) (2009) 12040–12047, http://dx.doi.org/10.1021/jp902684g.

[21] F. Fonseca, G. Goya, R. Jardim, N. Carreño, E. Longo, E. Leite, R. Muccillo, Magnetic properties of Ni : $SiO_2$ nanocomposites synthesized by a modified sol-gel method, Appl. Phys. A 76 (2003) 621–623, http://dx.doi.org/10.1007/s00339-002-2029-9.

[22] S.H. Masunaga, R.F. Jardim, P.F.P. Fichtner, J. Rivas, Role of dipolar interactions in a system of Ni nanoparticles studied by magnetic susceptibility measurements, Phys. Rev. B 80 (18) (2009) 184428, http://dx.doi.org/10.1103/PhysRevB.80.184428.

[23] B. Martinez, A. Roig, X. Obradors, E. Molins, A. Rouanet, C. Monty, Magnetic properties of $\gamma - Fe_2O_3$ nanoparticles obtained by vaporization condensation in a solar furnace, J. Appl. Phys. 79 (5) (1996) 2580–2586, http://dx.doi.org/10.1063/1.361125.

[24] J. Narayan, S. Nori, S. Ramachandran, J. Prater, The synthesis and magnetic properties of a nanostructured Ni – MgO system, JOM 61 (2009) 76–81, http://dx.doi.org/10.1007/s11837-009-0093-8.

[25] W.-N. Wang, G.-X. Cheng, Y.-W. Du, The interface magnetization of ultrafine Ni particles coated by NiO and Ni/NiO multilayers, J. Magn. Magn. Mater. 153 (1) (1996) 11–16, http://dx.doi.org/10.1016/0304-8853(95)00535-8.

[26] J.P. Chen, C.M. Sorensen, K.J. Klabunde, G.C. Hadjipanayis, E. Devlin, A. Kostikas, Size-dependent magnetic properties of $MnFe_2O_4$ fine particles synthesized by coprecipitation, Phys. Rev. B 54 (1996) 9288–9296, http://dx.doi.org/10.1103/PhysRevB.54.9288.

[27] R. Aquino, J. Depeyrot, M.H. Sousa, F.A. Tourinho, E. Dubois, R. Perzynski, Magnetization temperature dependence and freezing of surface spins in magnetic fluids based on ferrite nanoparticles, Phys. Rev. B 72 (2005) 184435, http://dx.doi.org/10.1103/PhysRevB.72.184435.

[28] C. Vázquez-Vázquez, M. López-Quintela, M. Buján-Núñez, J. Rivas, Finite size and surface effects on the magnetic properties of cobalt ferrite nanoparticles, J. Nanopart. Res. 13 (2011) 1663–1676, http://dx.doi.org/10.1007/s11051-010-9920-7.

[29] S. Mitra, K. Mandal, P. Anil Kumar, Temperature dependence of magnetic properties of $NiFe_2O_4$ nanoparticles embeded in $SiO_2$ matrix, J. Magn. Magn. Mater. 306 (2) (2006) 254–259, http://dx.doi.org/10.1016/j.jmmm.2006.03.024.

[30] A. Manukyan, A. Elsukova, A. Mirzakhanyan, H. Gyulasaryan, A. Kocharian, S. Sulyanov, M. Spasova, F. Römer, M. Farle, E. Sharoyan, Structure and size dependence of the magnetic properties of Ni@C nanocomposites, J. Magn. Magn. Mater. 467 (2018) 150–159, http://dx.doi.org/10.1016/j.jmmm.2018.07.056.

[31] P.W. Mitchell, D.M. Paul, Low-temperature spin-wave excitations in nickel, by neutron triple-axis spectroscopy, Phys. Rev. B 32 (1985) 3272–3278, http://dx.doi.org/10.1103/PhysRevB.32.3272.

[32] F. Zeb, K. Nadeem, S.K.A. Shah, M. Kamran, I.H. Gul, L. Ali, Surface spins disorder in uncoated and $SiO_2$ coated maghemite nanoparticles, J. Magn. Magn. Mater. 429 (2017) 270–275, http://dx.doi.org/10.1016/j.jmmm.2017.01.040.

[33] T.N. Shendruk, R.D. Desautels, B.W. Southern, J. van Lierop, The effect of surface spin disorder on the magnetism of $\gamma - Fe_2O_3$ nanoparticle dispersions, Nanotechnology 18 (45) (2007) 455704, http://dx.doi.org/10.1088/0957-4484/18/45/455704.

[34] M. Atif, M. Nadeem, M. Siddique, Cation distribution and enhanced surface effects on the temperature-dependent magnetization of as-prepared $NiFe_2O_4$ nanoparticles, Appl. Phys. A 120 (2015) 571–578, http://dx.doi.org/10.1007/s00339-015-9216-y.

[35] K. Chakrabarti, B. Sarkar, V.D. Ashok, K. Das, S.S. Chaudhuri, S.K. De, Interfacial magnetism and exchange coupling in $BiFeO_3$ – CuO nanocomposite, Nanotechnology 24 (50) (2013) 505711, http://dx.doi.org/10.1088/0957-4484/24/50/505711.

[36] K. Maaz, A. Mumtaz, S. Hasanain, M. Bertino, Temperature dependent coercivity and magnetization of nickel ferrite nanoparticles, J. Magn. Magn. Mater. 322 (15) (2010) 2199–2202, http://dx.doi.org/10.1016/j.jmmm.2010.02.010.

[37] D. Ortega, E. Vélez-Fort, D.A. García, R. García, R. Litrán, C. Barrera-Solano, M. Ramírez-del Solar, M. Domínguez, Size and surface effects in the magnetic properties of maghemite and magnetite coated nanoparticles, Phil. Trans. R. Soc. A 368 (1927) (2010) 4407–4418, http://dx.doi.org/10.1098/rsta.2010.0172.

[38] U. Khan, N. Adeela, K. Javed, S. Riaz, H. Ali, M. Iqbal, X. Han, S. Naseem, Influence of cobalt doping on structural and magnetic properties of $BiFeO_3$ nanoparticles, J. Nanopart. Res. 17 (2015) 1–9, http://dx.doi.org/10.1007/s11051-015-3233-9.

[39] P.V. Hendriksen, S. Linderoth, P.-A. Lindgård, Finite-size modifications of the magnetic properties of clusters, Phys. Rev. B 48 (1993) 7259–7273, http://dx.doi.org/10.1103/PhysRevB.48.7259.

[40] H. Kachkachi, A. Ezzir, M. Nogues, E. Tronc, Surface effects in nanoparticles: Application to maghemite-FeO, Eur. Phys. J. B 14 (2000) 681–689, http://dx.doi.org/10.1007/s100510051079.

[41] P.C. Rivas Rojas, P. Tancredi, C.L. Londoño-Calderón, O. Moscoso Londoño, L.M. Socolovsky, Comparison of the anisotropy energy obtained from temperature dependent AC and DC magnetometry in iron oxide nanoparticles (IONPs) with controlled dipolar interactions, J. Magn. Magn. Mater. 547 (2022) 168790, http://dx.doi.org/10.1016/j.jmmm.2021.168790.

[42] T. Prakash, G. Williams, J. Kennedy, S. Rubanov, $Ni_{1-x}Fe_x$ Nanoparticles made by low energy dual ion implantation into $SiO_2$, Mater. Res. Exp. 3 (12) (2016) 126102, http://dx.doi.org/10.1088/2053-1591/3/12/126102.

[43] G. Kopnov, Z. Vager, R. Naaman, New magnetic properties of silicon/silicon oxide interfaces, Adv. Mater. 19 (7) (2007) 925–928, http://dx.doi.org/10.1002/adma.200601762, arXiv:https://onlinelibrary.wiley.com/doi/pdf/10.1002/adma.200601762.

[44] C. Zhen, Y. Liu, Y. Zhang, L. Ma, C. Pan, D. Hou, Room-temperature ferromagnetism in Si – $-SiO_2$ composite film on glass substrate, J. Alloys Compd. 503 (1) (2010) 6–9, http://dx.doi.org/10.1016/j.jallcom.2010.04.226.

[45] P.J. Grace, M. Venkatesan, J. Alaria, J.M.D. Coey, G. Kopnov, R. Naaman, The origin of the magnetism of etched silicon, Adv. Mater. 21 (1) (2009) 71–74, http://dx.doi.org/10.1002/adma.200801098, arXiv:https://onlinelibrary.wiley.com/doi/pdf/10.1002/adma.200801098.

[46] C.M. Liu, X.L. Gao, Y. Zhang, L. Yang, Z.H. Yan, H.Q. Gu, X. Xiang, Y. Jiang, X.T. Zu, The microstructure, optical and magnetic property of nitrogen implanted $SiO_2$, Phys. Scr. 86 (2) (2012) 025703, http://dx.doi.org/10.1088/0031-8949/86/02/025703.

[47] D. Peddis, C. Cannas, G. Piccaluga, E. Agostinelli, D. Fiorani, Spin-glass-like freezing and enhanced magnetization in ultra-small $CoFe_2O_4$ nanoparticles, Nanotechnology 21 (12) (2010) 125705, http://dx.doi.org/10.1088/0957-4484/21/12/125705.

[48] W.H. Meiklejohn, C.P. Bean, New magnetic anisotropy, Phys. Rev. 102 (1956) 1413–1414, http://dx.doi.org/10.1103/PhysRev.102.1413.

[49] X. Batlle, M. García del Muro, J. Tejada, H. Pfeiffer, P. Görnert, E. Sinn, Magnetic study of M-type doped barium ferrite nanocrystalline powders, J. Appl. Phys. 74 (5) (1993) 3333–3340, http://dx.doi.org/10.1063/1.354558.

[50] R. Skomski, Nanomagnetics, J. Phys.: Condensed. Matter 15 (20) (2003) R841, http://dx.doi.org/10.1088/0953-8984/15/20/202.

[51] S.O. Demokritov, V.E. Demidov, O. Dzyapko, G.A. Melkov, A.A. Serga, B. Hillebrands, A.N. Slavin, Bose–Einstein condensation of quasi-equilibrium magnons at room temperature under pumping, Nature 443 (7110) (2006) 430–433, http://dx.doi.org/10.1038/nature05117.

[52] L.H. Bennett, E. Della Torre, P. Johnson, R. Watson, A phase diagram for the Bose-Einstein condensation of magnons, J. Appl. Phys. 101 (9) (2007) 09G103, http://dx.doi.org/10.1063/1.2696673.

[53] S. Chikazumi, Physics of Ferromagnetism, John Wiley & Sons, 1959.